Journal of Peptide Science
J. Peptide Sci. **11**: 215–224 (2005)
Published online 1 November 2004 in Wiley InterScience (www.interscience.wiley.com). DOI: 10.1002/psc.623

JOURNAL OF PEPTIDE SCIENCE

Simulation of the *N*-terminus of HIV-1 glycoprotein 41000 fusion peptide in micelles

ALLISON LANGHAM and YIANNIS KAZNESSIS*
Department of Chemical Engineering and Materials Science, University of Minnesota, MN 55455, USA

Received 13 May 2004; Revised 2 August 2004; Accepted 10 August 2004

Abstract: In this paper, the *N*-terminus of glycoprotein-41, the HIV-1 fusion peptide, was studied by molecular dynamics simulations in an explicit sodium dodecyl sulfate micelle. The simulation provides a detailed picture of the equilibrium structure and peptide stability as it interacts with the micelle. The equilibrium location of the peptide shows the peptide at the surface of the micelle with hydrophobic residues interacting with the micelle's core. At equilibrium, the peptide adopts an α-helical structure from residues 5–16 and a type-1 β-turn from 17–20 with the other residues exhibiting more flexible conformations. The primary hydrophobic interactions with the micelle are from the leucine and phenylalanine residues (Leu-7, Phe-8, Leu-9, Phe-11, Leu-12) while the alanine and glycine residues (Ala-1, Gly-3, Gly-5, Ala-6, Gly-10, Gly-13, Ala-14, Ala-15, Gly-16, Gly-10, Ala-21) interact favorably with water molecules. The results suggest that Phe-8, part of the highly conserved FLG motif of the fusion peptide, plays a key role in the interaction of the peptide with membranes. Our simulations corroborate experimental investigations of the fusion peptide in SDS micelles, providing a high-resolution picture that explains the experimental findings.

Keywords: membrane mimics; sodium dodecyl sulfate; GP41; fusion peptide; molecular dynamics simulation; micelles; peptide membrane interactions

INTRODUCTION

Envelope viruses such as HIV and influenza infect cells by binding to the cell membrane and then fusing the viral envelope membrane with the target cell membrane. In general, one protein in the virus is responsible for the membrane fusion step of this process. The essential step in the viral infection of cells is the insertion of this protein into the target cell membrane. Therefore, it is vitally important to understand the mechanism of insertion, particularly the sequence and structure of the fusion protein as it penetrates and destabilizes the membrane. For type-1 HIV, the segment responsible for fusion with the host cell membrane is located at the *N*-terminus of the fusion peptide [1]. This fusion peptide, gp160, is composed of two noncovalently associated subunits: gp120, a surface glycoprotein and gp41, a transmembrane glycoprotein. The subunit gp120 binds to the CD4 receptor and to chemokine co-receptors on the target cell while gp41 promotes fusion of viral and cellular membranes. Combined, these two actions lead to entry into the cell and transport of the viral core to the nucleus, ultimately leading to viral expression in the cell [2].

It is important to study the *N*-terminus of HIV-1 gp41 (FP, A V G I G A L F L G F L G A A G S T M G A R S) because of its participation in HIV-1 transmission. It is particularly important to determine the exact structure of FP in aqueous and membrane interface environments [3–5]. The interaction of the peptide with the membrane and the conformation that the peptide adopts as it interacts with the membrane play an important role in the path to peptide-target cell binding. FP has been studied through experimental methods such as circular dichroism and Fourier transform infrared spectroscopy. These studies have shown FP to contain varying amounts of α-helix, β-sheet and random conformation in different membrane mimics.

Mobley and coworkers investigated the role of gp41 in human erythrocyte fusion, and demonstrated that the *N*-terminus of gp41 plays a critical role in fusion and cytopathic processes causing HIV-1 infection of target cells [6]. Chang and coworkers found that the FLG motif of gp41 appears to be essential in inducing lysis of lipid vesicles and that the peptide adopts a predominately helical structure with A15-G16 being positioned at the micelle-water interfaces [3]. Vidal and coworkers hypothesized that for FP in SDS micelles, the structured domains involve the hydrophobic residues, while the hydrophilic residues are disordered. They also proposed that the β-sheet conformational state plays the major role in membrane translocation [7]. The structure of FP in SDS was predicted via FTIR and CD to be predominately α-helix [4]. In addition, methods such as electron spin resonance with spin labeled fusion peptide have been used to define the conformation and topography of FP in membrane mimics [3]. FTIR and CD provide general information about the structure of FP; however, these are global methodologies and therefore cannot assign orientations to specific residues.

*Correspondence to: Dr Yiannis Kaznessis, Department of Chemical Engineering and Materials Science, University of Minnesota, 421 Washington Avenue, SE, Minneapolis, MN 55455, USA;
e-mail: yiannis@cems.umn.edu

Recently, Gordon and coworkers have investigated FP in SDS using conventional ^{12}C-FTIR and ^{13}C-enhanced FTIR to define specific conformations of FP in aqueous membrane mimic environments [8].

Molecular dynamics simulations have been shown to be particularly successful in providing an atomistic picture of the interaction of peptides with membrane mimics such as SDS micelles. Wymore has studied the interactions of adrenocorticotropin (ACTH) in solvated SDS micelles and succeeded in determining the equilibrium conformation [9]. Additionally, for ACTH, Wymore demonstrated through MD simulations that the membrane can induce secondary structure changes in the peptide that may facilitate the peptide-receptor recognition process and were able to provide clear information on these changes [10].

This work investigates the interaction of the *N*-terminus of gp41, FP, with a SDS micelle using molecular dynamics simulations. The system examined consisted of one SDS micelle and one FP molecule in water. The goal of the study was to provide a clear atomistic level picture of the structure of FP during interactions with membrane mimics and its relative position to the interface. This, combined with previous experimental data, will answer questions about the stability of FP in such environments and clarify the implications of the secondary structure on fusion peptide activity.

METHODS

The simulation of FP in a SDS micelle was performed using CHARMM version c28b2 [11]. Water was modeled using TIP3P [12]. The system was composed of more than 16 000 atoms: 4375 water molecules, 60 SDS molecules, the peptide, 0.15 mM NaCl and necessary counterions. The SDS micelle was built using MacKerell's method [13]. In this method, the molecule buckminsterfullerene is used as a model to ensure equal distribution of the sulfate head groups over the surface of the micelle. The dodecyl sulfate C12 methyl carbons were placed 3.0 Å from the center of the fullerene structure and the molecules were built outward by placing the carbons in an all-*trans* configuration, based on the geometries included in the CHARMM all hydrogen lipid parameter set. Systematic body rotations of SDS molecules were used to perform a global search and to reduce the number of unrealistic hard-core overlaps. Energy minimizations were performed, allowing the internal degrees of freedom of the molecule to relax, resulting in a spherical micelle of radius 23.3 Å (measured as the average distance from the center of mass of the micelle to the sulfur atoms of the head group).

The initial conformation of the peptide in DPPC was obtained from the Protein Data Bank (PDB accession code: 1ERF; www.rcsb.org). Although the structure of FP in DPPC is not assumed to be identical to the equilibrium structure of FP in SDS, it provides a very good starting point. According to the conclusions drawn by Chang, FP is largely embedded in the micelle [3]. Specifically, residues 1–15 are shown to be inside the micelle's core in a configuration modeled by Chang [3]. In the simulations, the peptide was initially inserted with its α-helical axis (Ile-4 to Ala-15) overlapping the axis of one of the SDS molecules [3]. This view is shown in Figure 1. The *N*-terminus of the peptide was inserted into the core of the micelle, with the C-α atom of Ala-15 overlapping the sulfur atom of a SDS molecule, leaving the *C*-terminus outside the micelle. The initial position was chosen based on the hypothesis from Chang, which suggested that the equilibrium position of FP in SDS is in the center of the micelle [3]. The insertion led to a number of unrealistic overlaps ('bad

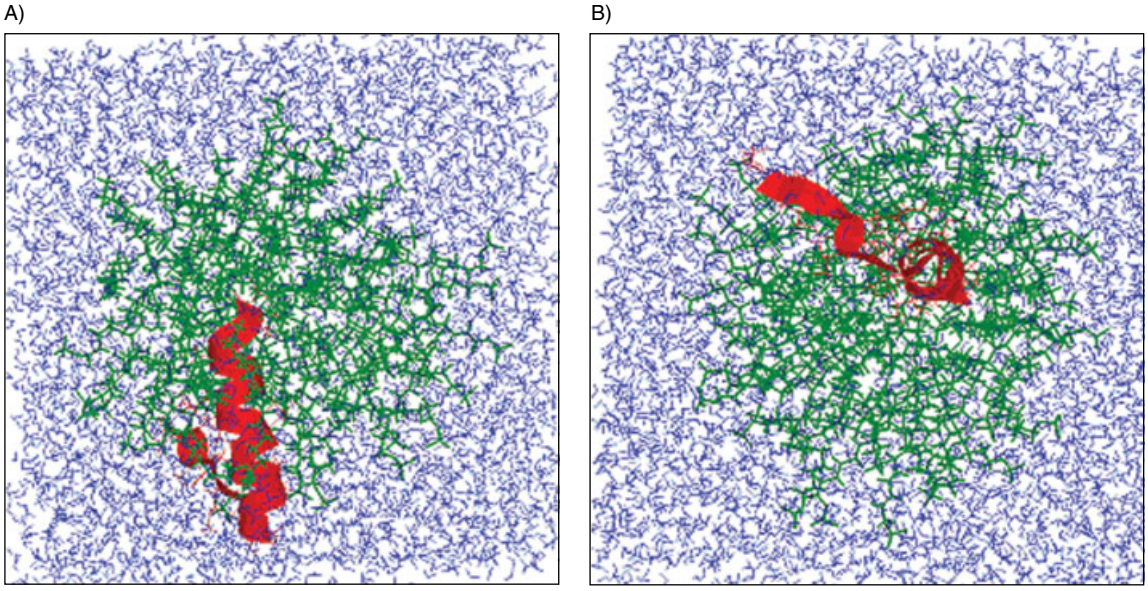

Figure 1 Configuration of the system after energy minimization and heating. FP is displayed as a red ribbon, SDS in green and water in blue. (A) side view of the peptide as it is inserted into the center of the micelle, (B) micelle from the top along the axis of the helix. The initial conformation of the peptide was obtained from the PDB, accession code 1ERF. The position of the peptide in the micelle was suggested as the equilibrium location by Chang [3].

contacts'), which were defined as a distance between two non-hydrogen atoms of less than 2.3 Å. The SDS molecules were systematically rotated and translated, with the peptide kept stationary, and in order to reduce the number of overlaps, a second energy minimization was performed. The peptide–SDS micelle complex was then solvated in a cube of side length 54.141 Å with 4375 TIP3P water molecules. Finally, 0.15 M NaCl was added to the water region, as well as counterions, in order to neutralize the charge of the system.

The entire system was minimized in 2000 steps of steepest descent and heated to 303.15 K in 500 ps. The system was allowed to equilibrate at constant temperature and pressure for another 500 ps. The resulting system is presented in Figure 1. The constant temperature-pressure module of CHARMM was used for the simulation with a leapfrog integrator using a 2 fs time step. The temperature was held constant at 303.15 K by the Hoover temperature control with a thermal piston mass of 1500 kcal. For the extended system pressure algorithm employed, all components of the piston mass array were set to 500 amu [14]. The nonbonded van der Waals interactions were switched off smoothly between 9 Å and 12 Å. The electrostatic interactions were simulated using the particle mesh Ewald (PME) summation with no truncation [15]. A real space Gaussian width of 0.42 A^{-1}, a B spline order of 6, and a FFT grid of about one point per Å were used. The SHAKE algorithm was used to hold the hydrogen bonds fixed [16]. Periodic boundary conditions were applied in all dimensions.

The properties were calculated using the data from the trajectory files created by CHARMM. Based on pressure and total energy data, the system is considered in equilibrium from 1.3 ns to 2.5 ns (Figure 2). Before this, the peptide is moving out of the micelle as mentioned in results and detailed in the discussion, and the data from this portion of the simulation are not included in calculations of electron density profiles or pair distribution functions. For dihedral angle calculations, data from 0.2 ns to 2.5 ns are included, to obtain a better picture of the flexibility of the peptides. Values for the angles were also calculated for 0.2 to 0.4 ns and 2.3 to 2.5 ns to determine changes in the secondary structure of the peptide from the initial conformation (that of FP in HFIP) to its final equilibrium conformation.

The first observation to be made was the migration of the peptide during the simulation. At the beginning of the simulation, the peptide was clearly positioned with the *N*-terminus in the center of the micelle with the *C*-terminus outside the micelle. Within the first 1 ns of simulation the peptide had diffused from the core to the surface of the micelle. The final location of the peptide is shown in Figure 3. In addition to the diffusion, the peptide also changed structure, the α-helix becoming partially unraveled.

RESULTS

Dihedral Angles

The dihedral angles Φ and Ψ were calculated from 0.2 to 2.5 ns and the average and root mean square deviations

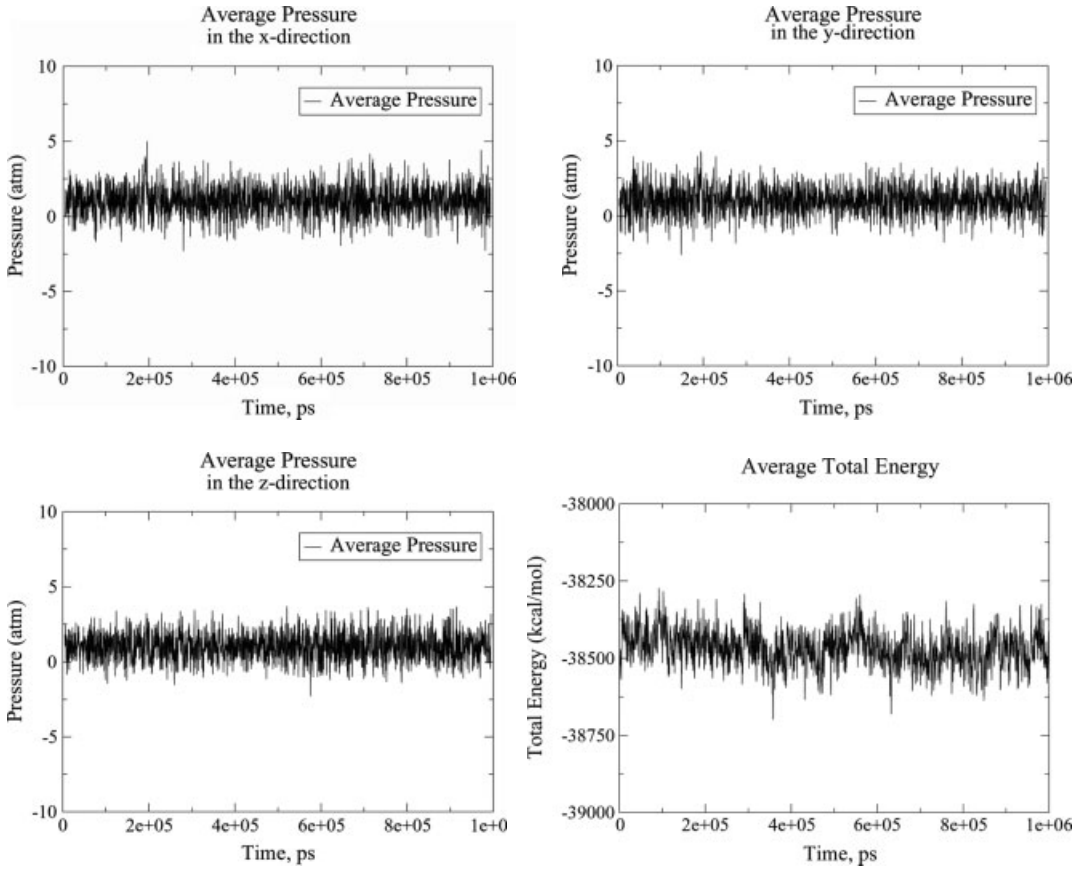

Figure 2 Average pressure and total energy data. Averages calculated over 20 ps intervals. Time step 0 is equivalent to time 0.2 ns, after minimization and heating.

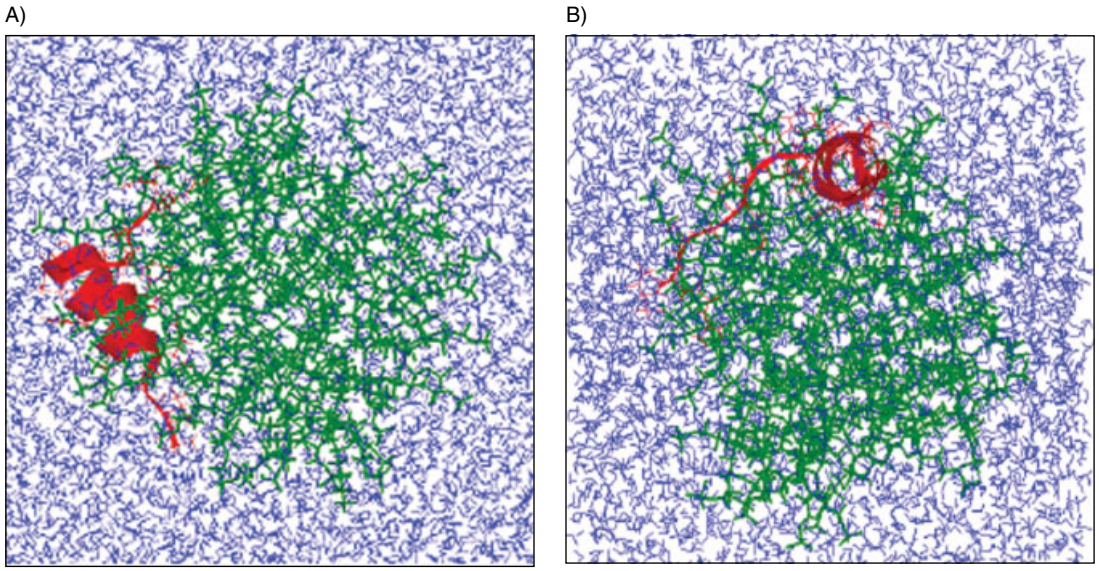

Figure 3 The system at 2.5 ns, when the peptide has moved to the surface of the micelle. The α-helix has unfolded partially to contain only three turns, with one side facing the micelle and the other facing away from the micelle surface. The conformation shown has been deposited into the PDB under accession code 1P5A.

Table 1 Average Φ-Ψ Values (in degrees) for FP in a SDS Micelle in Water with RMSD Fluctuations in Parenthesis, based on the data from 0.2 ns to 2.5 ns

Amino acid	Φ	Ψ
Val-2	−88.2 (18.2)	68.2 (143.0)
Gly-3	−87.2 (25.9)	68.6 (25.1)
Ile-4	−70.8 (11.1)	−48.4 (9.8)
Gly-5	−67.61 (10.6)	−37.9 (11.4)
Ala-6	−60.8 (10.2)	−45.7 (11.5)
Leu-7	−69.3 (10.4)	−62.9 (8.4)
Phe-8	−72.8 (9.1)	−52.9 (10.1)
Leu-9	−78.6 (10.2)	−45.1 (11.1)
Gly-10	−75.8 (12.6)	−66.7 (11.6)
Phe-11	−72.7 (11.3)	−53.1 (9.0)
Leu-12	−76.8 (9.4)	−45.5 (13.0)
Gly-13	−77.7 (14.0)	−69.2 (12.2)
Ala-14	−73.0 (11.4)	−51.8 (10.5)
Ala-15	−71.5 (9.4)	−50.4 (15.8)
Gly-16	100.8 (18.6)	54.9 (20.3)
Ser-17	−88.8 (19.0)	126.0 (89.9)
Thr-18	−90.4 (17.1)	129.7 (12.9)
Met-19	−82.6 (12.4)	−66.9 (15.4)
Gly-20	17.0 (155.6)	16.0 (155.3)
Ala-21	−115.5 (28.6)	122.0 (86.7)
Arg-22	−94.0 (17.9)	9.8 (119.7)
Ser-23	−89.4 (21.9)	−89.4 (21.9)

for each angle over this time (RMSD) were calculated. Table 1 gives the value of Φ and Ψ with RMSD values. Figure 4 shows a plot of these values. The residues from 4–15 exhibit dihedral angles typical of an α-helix with little variation throughout the simulation, suggesting

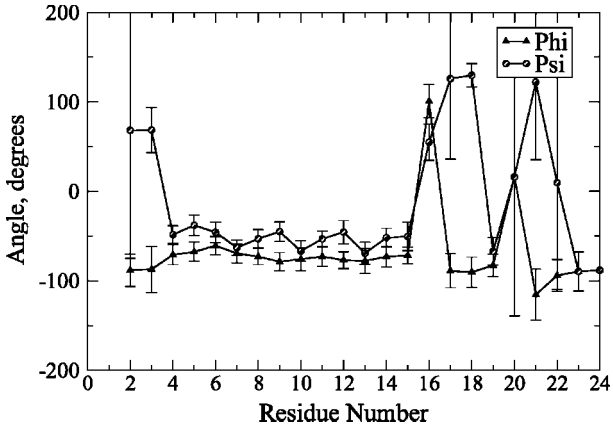

Figure 4 Average Φ-Ψ values for FP in a SDS micelle in water. Averages calculated over 0.2 to 2.5 ns.

that this region of the FP forms an α-helix and remains in this conformation during its interactions with the SDS micelle.

Residues 1–4 exhibit random conformations throughout the simulation. Residues 17 and 18 are consistent with extended conformation, but have high RMSD values, suggesting that their conformation fluctuates throughout the simulation. Based on the angle values at the end of the simulation, these residues stabilize as extended conformation. The residues from Ser-17 to Gly-20 exhibit a type 1 β-turn, a set of certain dihedral angles and a distance between two of the residues of less than 7 Å.

The residues in the *C*-terminal region of FP (residues 20–23) do not exhibit a constant conformation, but rather fluctuate during the simulation, particularly in Ψ. This region of the peptide was observed to

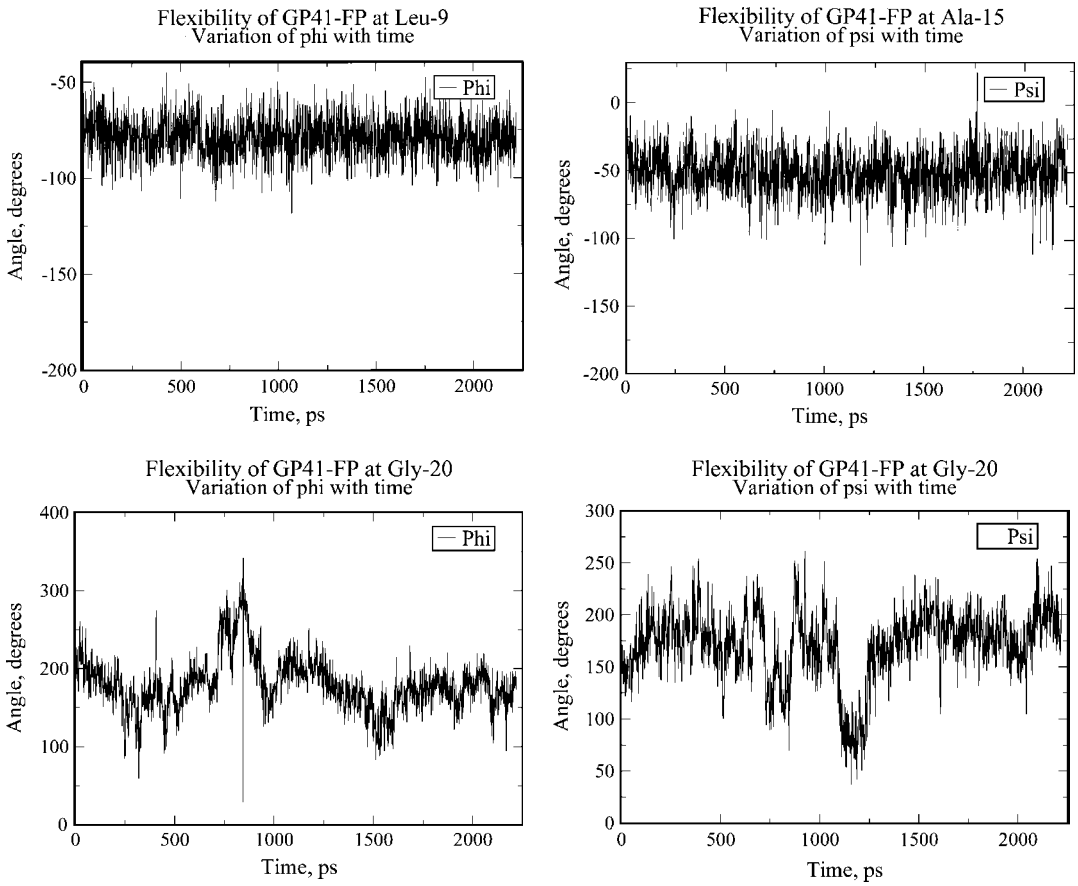

Figure 5 Selected plots of Φ and Ψ from 0.2 ns to 2.5 ns. Leu-9, located in the α-helix, exhibits little variation over time. The residues near the *C*-terminal end of FP exhibit much greater flexibility.

move a great deal during the simulation. At Gly-20, in particular, the peptide exhibits a high degree of flexibility throughout the simulation. The RMS value over the 2.3 ns range listed in Table 1 is comparatively high, but RMS values calculated over the first 0.2 ns after heating and for the final 0.2 ns of simulation show RMS values of up to 10 times that of the other residues (Φ: −56.5° (151.9); Ψ: 71.6° (142.4)). As seen in Figure 5, which shows selected plots of the value of dihedral angles at specific amino acids, the peptide is particularly flexible in Ψ at residues 2, 17, 20, 21 and 22. The *C*-terminal end of FP, therefore does not consistently remain in any conformation, but is highly flexible.

Pair Distribution Functions

Pair distribution functions were calculated for the carbonyl group on each residue with the bulk water. Using CHARMM, the number of water molecules at a distance of less than 15 Å from the carbonyl of the backbone residue was determined with incremental distances of 0.2 Å. The data were averaged over the last 500 ps of the simulation. Plots showing the results of the pair distribution functions for representative residues are shown in Figure 6. Analysis of these data confirms the amphipathic nature of FP previously reported.

The glycine and alanine residues (Ala-1, Gly-3, Gly-5, Ala-6, Gly-10, Gly-13, Ala-14, Ala-15, Gly-16, Gly-20 and Ala-21) show a significant peak around 2.7 Å. Hydration numbers were calculated for the residues at this radius and the results are listed in Table 2. Additionally, the residues at the *C*-terminal end of FP exhibit attraction to water; these residues include Ser-17–Ser-23. While the hydration numbers for residues 17–23 are relatively low, these residues can be considered hydrophilic based on their location away from the micelle surface.

The leucine and phenylalanine residues (Leu-7, Phe-8, Leu-9, Phe-11 and Leu-12) along with Ile-4 do not have the characteristic peak at 2.7 Å and are therefore considered hydrophobic. Their hydration numbers at this radial distance are nearly zero.

FP has alternating sections of hydrophilic and hydrophobic residues, which, when considered with the α-helical structure, confirms previous evidence of a 'glycine stripe' on the α-helix. This region includes all the glycine and alanine residues, excluding Gly-20 and Ala-21. It occupies one full side of the helix as pictured in Figure 7. This model is of interest as it is the same structure that has been noted in HFIP by ^{13}C-FTIR

Table 2 Hydration Numbers for All Residues at a Radial Distance of 2.7 from the Carbonyl of the Residue

Amino acid	Hydration number at 2.7 Å
Ala-1	0.980
Val-2	0.281
Gly-3	0.023
Ile-4	0.000
Gly-5	0.003
Ala–6	0.034
Leu-7	0.000
Phe-8	0.000
Leu-9	0.034
Gly-10	0.186
Phe-11	0.183
Leu-12	0.415
Gly-13	0.607
Ala-14	0.905
Ala-15	0.975
Gly-16	0.951
Ser-17	0.508
Thr-18	0.536
Met-19	0.368
Gly-20	0.336
Ala-21	0.395
Arg-22	0.429
Ser-23	0.443

analysis [5]; however, in more polar solvents, such as TFE, this stripe deteriorates into a predominately random conformation, likely due to the effect of solvent on the stripe.

Electron Density Profiles

Electron density profiles were calculated for each major functional group in the system: the methyl groups, the carbon chains and the sulfate head groups of SDS; the water, sodium and chlorine; and each residue of the peptide. Electron density profiles were calculated using CHARMM based on the radial distance from the center of the simulation box averaged over the last 500 ps, which corresponds to the center of the micelle, outward. In each differential element of the sphere, the number of each species was calculated. These data are readily converted to electron density by multiplying by the number of electrons for the atom or molecule and dividing by the volume of the spherical shell.

The profiles of the system are shown in Figures 8–10. In Figure 8, the residues that were suggested to be hydrophobic by the pair distribution functions were plotted to determine their location relative to the micelle surface. These residues are located between the carbon chains on the SDS and the sulfate head groups, suggesting that they are located near the inside surface

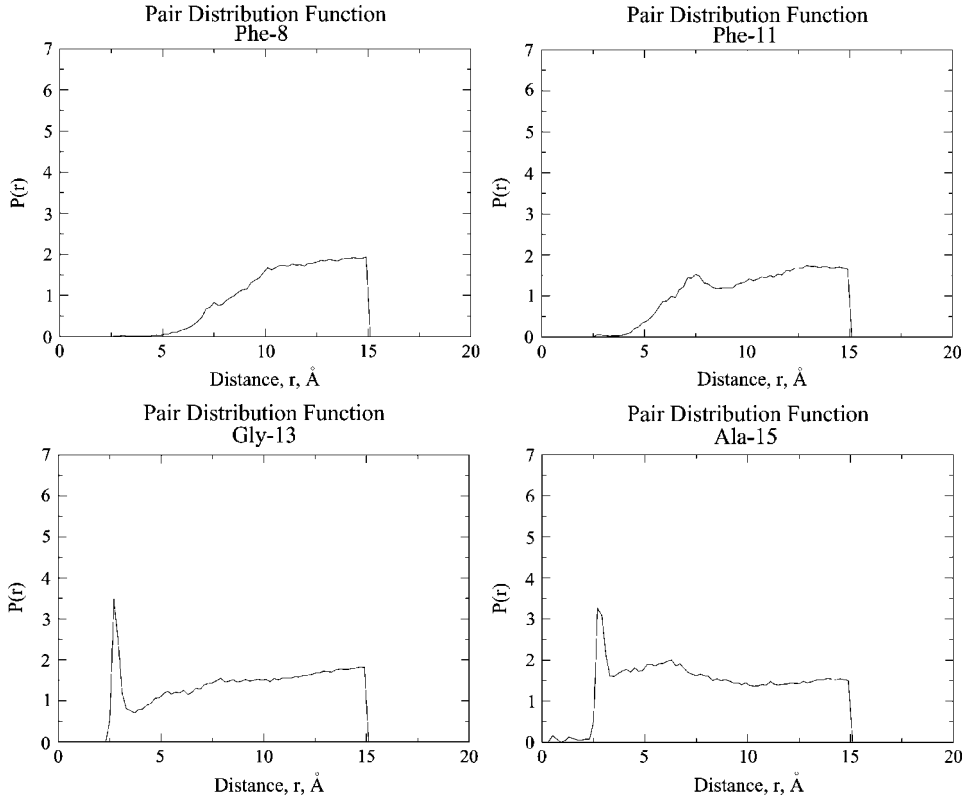

Figure 6 Pair distribution functions of selected, representative carbonyl oxygen atoms of the peptide with oxygen atoms of water calculated for a distance of 15 Å from the atom. Shown are hydrophobic residues Phe-8 and Phe-11, along with hydrophilic residues Gly-13 and Ala-14.

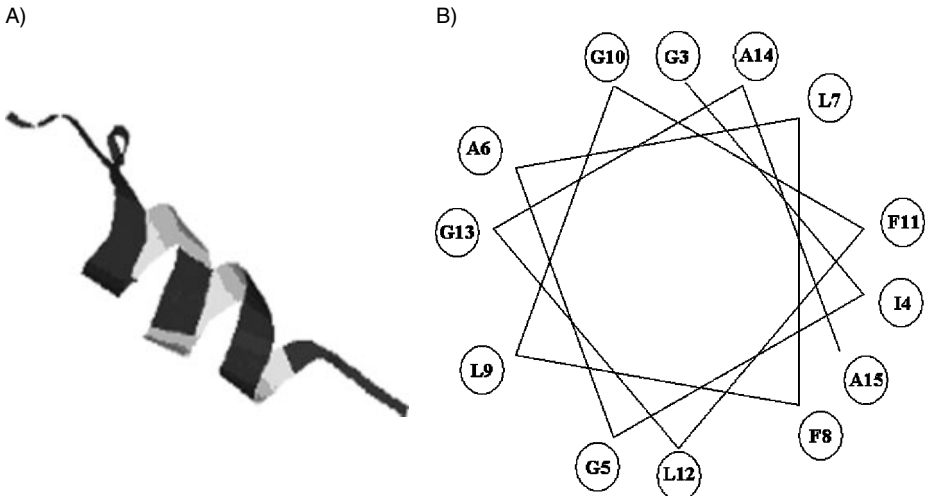

Figure 7 Image of FP showing the amphipathic nature of the peptide. Hydrophobic residues are light and hydrophilic residues are dark. The dark stripe along the helix is the 'glycine stripe'. B shows the helical wheel for residues 3 through 15.

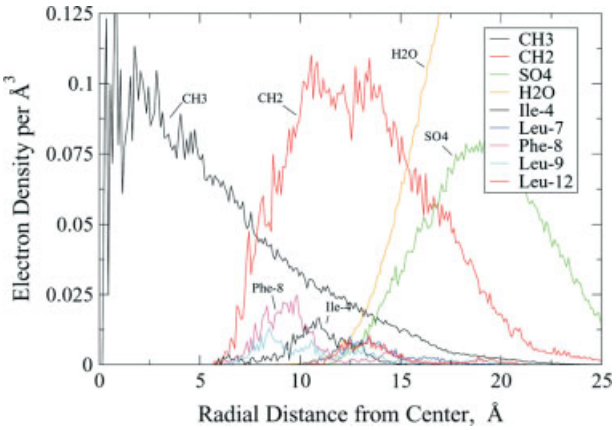

Figure 8 Electron density profile for the FP-SDS system, showing the hydrophobic residues. The residues are located primarily at a radial distance from the center of the simulation box of less than 15 Å.

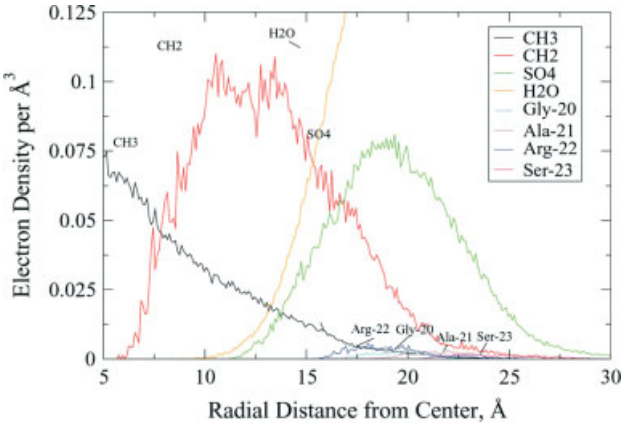

Figure 9 Electron density profile for the FP-SDS system, showing the primarily hydrophilic residues of the *C*-terminal region of FP. These residues are located a radial distances greater than 15 Å from the center of the simulation box.

of the micelle. Phe-8 appears to be located farthest inside the micelle.

In Figures 9 and 10, the electron density profiles of the hydrophilic residues are plotted. These residues are located between the sulfate head groups and bulk water, suggesting that these groups are on the regions of the peptide facing the water as opposed to the micelle surface. The residues plotted in Figure 9 are the residues that compose the *C*-terminal end of FP. As was suggested from the simulation images, these residues reside in the water, away from the micelle surface for the majority of the simulation. Figure 10 shows the members of the 'glycine stripe', which electron density data support as being hydrophilic and located facing away from the SDS micelle surface toward the water.

As can be observed in Figures 8, 9 and 10, groups with peaks located more than 15 Å from the center of the simulation box in the electron density profiles are the groups that are located on the side of the α-helix that faces the water and section of the residue in water, while the groups that are less than 15 Å from the center are located on the region of the α-helix near the micelle surface. Gly-20, Ala-21, Arg-22 and Ser-23 are located the farthest from the center, as shown in Figure 9. These groups make up the *C*-terminal end of FP and exhibit more motion than the other residues during the course of the simulation.

DISCUSSION AND CONCLUSION

The purpose of this molecular dynamics simulation study was to provide a clear understanding of the interactions of FP with a micelle at the atomistic level. The results can be compared with several laboratory studies of FP; in particular, a recent study by Gordon and coworkers [8].

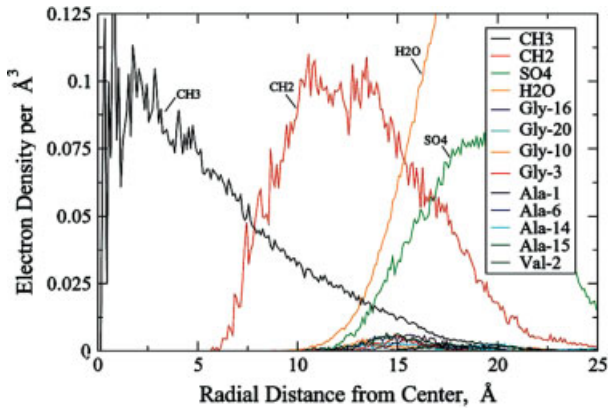

Figure 10 Electron density profile showing the residues that compose the 'glycine stripe'. These hydrophilic residues are located at radial distances greater than 15 Å from the center of the simulation box.

The equilibrium conformation of FP in the SDS micelles suggested by the simulation is one in which residues 1–4 and residues 16–23 are located outside the micelle in the bulk water. Residues 5–15 form an amphiphilic α-helix. The hydrophobic side of the helix is located on the surface and inside the micelle. The hydrophilic side faces away from the micelle surface. What is remarkable is that although the peptide's initial configuration is at the center of the micelle, within 1 ns, the peptide has reached its equilibrium location.

Chang and co-workers draw three conclusions about the location of FP in a SDS micelle [3]. The first, from NMR, CD and electron paramagnetic resonance experiments suggests that the *N*-terminus, residues 1–4, is located outside the micelle interior. Second, from similar experiments, is that the *C*-terminus, residues 15–23, is also located outside the micelle interior with residues Ala-15 and Gly-16 positioned at the interface. Both of these are corroborated by simulation results. The third conclusion is based on fluorescence measurements with Trp-8 substituted in place of Phe-8, which indicated Trp-8 interacting with the core of the micelle. Chang and co-workers propose that the helical coil from residue 5–14 is located in such a manner that Phe-8 is at the center of the micelle interior [3]. This, however, is not geometrically possible. The peptide, in its predominantly helical conformation, is not long enough to span the diameter of the micelle and have the *N* and *C* termini outside the micelle and residue 8 near the center. The location of the α-helix with respect to the micelle is the main point of disagreement between the simulation results and the results discussed by Chang and co-workers. The simulation shows that residues 8–11 (the FLG motif) are located in the micelle interior; however, residues 5–8 and 11–15 are located at the micelle surface or in the bulk water. The hydrophilic portions of the helix are arranged so that they are facing outward toward the bulk water. In agreement with Chang's results, residue Phe-8 is inserted the furthest into the micelle, however, the simulation results propose a more reasonable location for the peptide with respect to the micelle that allows for exposure of the *N* and *C* termini to the bulk water. It is proposed that Phe-8 is not in the center of the micelle, but simply in the interior of the micelle and that the other helical residues are then located near the surface of the micelle, with hydrophobic residues facing the interior and hydrophilic residues facing the water, but interacting with the micelle. The simulation results, which are in agreement with the experimental results, provide an alternative and more plausible interpretation in terms of the position of the peptide.

The results from the calculation of the dihedral angles support the structure recently proposed by Gordon and coworkers [8]. Based on ^{13}C-enhanced FTIR, they reported the following levels of secondary structures in FP in SDS: 44% α-helical, 23% β-sheet, 21% β-turn and 12% disordered. Chang and coworkers report 58.9% α-helix, 11.4% β-sheet, 15.2%β-turn and 15.3% others from CD data [3]. The values determined from this study, 55% α-helical, 9% β-sheet, 18% β-turn and 18% disordered, agree qualitatively with both sets of data.

Gordon and coworkers also predicted the following conformational map for FP in SDS micelles: random or disordered structures from residues 1–4, α-helix from residues 5–16, and random and minor β-sheet for residues 17–23 [8]. The results from the simulation agree on the conformation of the first 15 residues, disordered until residue 4 followed by a α-helix. The simulation also agrees on the presence of a β structure in residues 17–20 with the remaining residues in random conformations.

Both Chang [3] and Gordon [8] have noted the possible importance of the Ala-15–Gly-16 segment. Gordon proposes that this segment acts as a glycine cap terminating the α-helix [8]. Chang further suggests that this segment is a transition between the solvent exposed *C*-terminal portion and the micelle embedded *N*-terminus [3]. From their studies in SDS, this region is also a link between two helical regions, from Ile-4 to Ala-15 and Gly-16 to Arg-22 [3]. While there is not agreement that the segment links two helical regions as the simulation shows β-turn for residues 17–20, the simulation results do agree on the existence of a glycine cap at Ala-15 that marks the end of the helical region and a transition to a more flexible region. Chang suggests that because the two residues are located at the micelle boundary, they may affect biological function [3]. Our findings do show A15–G16 as the residues marking a clear boundary for the peptide between micelle and water, but electron density data do put the cap near the surface of the micelle. We propose that the cap plays an important role in mediating the interactions between the viral envelope and the cell membrane. FP attaches itself to the cell membrane at the glycine cap and this provides an anchor to allow

the *N*-leucine zipper to act on the target cell. The cap is located at the surface of the micelle and positions the helix on the surface to allow interaction between the viral envelope and target cell necessary for infection.

Disorder at the *N*-terminus of FP is also supported by simulation data, as no specific secondary structure is suggested from the dihedral angles. The peptide is particularly flexible around Val-2. Kamath also noted the conformational flexibility of the region from residues 1–5, and proposed that it may play an important role by allowing the peptide to insert into a bilayer by reorienting itself [17]. This is in agreement with the movement of the peptide from its original conformation and position in the micelle to its equilibrium position. In the simulation, the *N*-terminus also moves very quickly from the center of the micelle to the bulk water. This is likely due to the unsatisfied hydrogen bonds when the peptide is located in the micelle interior. As can be seen in Figure 11, the number of hydrogen bonds between residues 1–4 and the bulk water and SDS head groups increases very early in the simulation, from none to an average of nearly 5, as the *N*-terminus moves out of the micelle in the first few hundred picoseconds.

The original structure was obtained by Gordon and coworkers in hexafluoroisopropanol (HFIP) [5]. According to ^{13}C-FTIR spectroscopy and energy minimizations of FP in HFIP, residues 3–16 fold as a α-helix. In the final structure at equilibrium in SDS, residues 1–5 are disordered, and the α-helix does not include residues 1–4, supporting the speculation that the flexibility of these *N*-terminal residues is important for insertion. However, it has been suggested that this disorder is due to SDS in particular, as residues 1–4 are generally α-helix in other membrane mimics [8]. The region from residues 5–15 may be more involved in the actual lysis of a membrane, requiring the flexibility seen for the segments 1–4 and 16–23.

FTIR spectra of FP with ^{13}C-carbonyls at Gly-20 and Ala-21 indicate that Gly-20 and Ala-21are β-sheet [8].

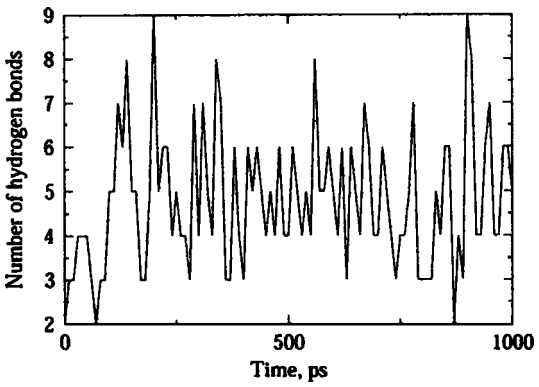

Figure 11 The evolution of the number of hydrogen bonds with time for the *N*-terminus of FP, residues 1–4. There is an increase in the number of bonds due to the movement of the peptide out of the micelle interior.

The simulation predicts a similar amount of extended conformation, approximately 20%; however, it gives the location of this at Ser-17 and Thr-18.

The analysis of pair distribution functions between the carbonyl group of each residue with water support the conclusion that FP exhibits an amphipathic nature. It has been shown, from both simulation data and ^{13}C-FTIR spectra, that FP in SDS folds itself in an amphipathic α-helix, with a hydrophobic side and a more hydrophilic side that includes the 'glycine stripe' (i.e. Gly-3, Gly-5, Gly-10, Gly-13, Ala-14, Ala-15 and Gly-16). This corroborates Mobley's findings that the peptide forms a hydrophobic–hydrophilic segregated helix [18].

The FLG motif has been of particular interest in the study of FP. Chang observes that the F8-G10 segment forms a type 1 β-turn in water, and is thought to be the initiation site for helix formation of the peptide when introduced to SDS micellar solution [19]. Kamath also noted that this residue might be important in contributing to peptide insertion [17]. Phe-8 is thought to be essential in inducing lysis of lipid vesicles. Chang studied the immersion of F8 into the micellar interior by substituting phenylalanine with tryptophan [3]. By fluorescence and EPR experiments, he showed that the side chain of W8 penetrated the hydrocarbon interior of a bilayer by at least 7 Å. Molecular dynamics simulations also propose that Phe-8 will be buried in the micelle interior. It is the most hydrophobic residue, as noted by its pair distribution function with water and its hydration number. The simulation data support Chang's hypothesis as correct and that this residue may play an important role in the fusogenic process.

Gordon and coworkers noted that FP significantly perturbed the SDS micellar organization, and proposed that this behavior is suggestive of its fusogenic action [8]. While it is difficult to quantify from the properties calculated whether this is true, from observing the interactions of FP with the micelle during the simulation, it is clearly noted that the micelle is perturbed and it follows that this is likely due to the fusogenic action of FP. In viewing the simulation, it is clear that the micelle exhibits shape fluctuations, likely due to perturbations from the peptide. In addition to disrupting the micelle, FP undergoes alterations as it migrates from the micelle core to the surface. Also noted is the 'fraying' of the *N*-terminus. The helix remains intact for the mid-portion of the peptide; however, the *N*-terminus and *C*-terminus unravel.

In conclusion, the results of the quantitative analysis of the MD simulation of FP in a SDS micelle agree with many of the previous studies of the same system by physical techniques. The simulation gave a high-resolution image of the system, from which the conformation FP adopts in SDS can be specifically determined. The FP molecule is predominately α-helical, from residues 4–15, with extended conformation also

represented at locations in the peptide. The *N*-terminal and *C*-terminal regions of FP are disordered in SDS.

Future work can be conducted on FP by simulation to determine how it behaves in other membrane mimics. Also, just as altered FP has been studied via traditional laboratory techniques, simulations of the interactions of these altered FP molecules, with different groups in significant locations, could be performed and analysed to compare the effects site-directed mutagenesis have on the interaction of FP with a SDS micelle or other membrane mimics. Such simulations would provide similarly high-resolution images, which may provide a better understanding of the mechanism by which HIV-1 enters human cells, ultimately leading to the development of antiviral peptides to inhibit the ability of HIV to infect cells.

Acknowledgements

This work was partially supported by the National Institute of Biomedical Imaging and Bioengineering and the National Science Foundation (EEC- 0234112) through a University of Minnesota Bioinformatics Summer Institute fellowship to Allison Langham.

Computer resources support from the Minnesota Supercomputing Institute and the National Center for Supercomputing Applications (grant: MCB020026N) is gratefully acknowledged.

REFERENCES

1. McCune JM, Rabin LB, Feinberg MB, Lieberman M, Kosek JC, Reyes GR, Weisman IL. Endoproteolytic cleavage of gp160 is required for the activation of human immunodeficiency virus. *Cell* 1988; **53**: 55–67.
2. Kilby JM, Hopkins A, Venetta TM, DiMassimo B, Cloud GA, Lee JY, Alldredge L, Hunter E, Lambert D, Bolognesi D, Matthews T, Johnson MR, Nowak MA, Shaw GM, Saag MS. Potent suppression of HIV-1 replication in humans by T-20, a peptide inhibitor of gp41-mediated virus entry. *Nat. Med.* 1998; **4**: 1302–1307.
3. Chang D-K, Cheng S-F, Chien W. The amino-terminal fusion domain peptide of human immunodeficiency virus type 1 gp41 inserts into the sodium dodecyl sulfate micelle primarily as a helix with a conserved glycine at the micelle-water interface. *J. Virol.* 1997; **9**: 6593–6602.
4. Mobley PW, Waring AJ, Sherman MA, Gordon LM. Membrane interactions of the synthetic *N*-terminal peptide of HIV-1 gp41 and its structural analogs. *Biochim. Biophys. Acta* 1999; **1418**: 1–18.
5. Gordon LM, Mobley PW, Pilpa R, Sherman MA, Waring AJ. Conformational mapping of the *N*-terminal peptide of HIV-1 gp41 in membrane environments using (13)C-enhanced Fourier transform infrared spectroscopy. *Biochim. Biophys. Acta* 2002; **1559**: 96–120.
6. Mobley PW, Lee H-F, Curtain CC, Kirkpatrick A, Waring AJ, Gordon LM. The amino-terminal peptide of HIV-1 glycoprotein 41 fuses human erythrocytes. *Biochim. Biophys. Acta* 1995; **1271**: 304–314.
7. Vidal P, Chalion L, Heitz A, Van Mau N, Mery J, Divita G, Heitz F. Interactions of primary amphipathic vector peptides with membranes: conformational consequences and influence on cellular localization. *J. Membrane Bio.* 1998; **162**: 259–264.
8. Gordon LM, Mobley PW, Lee W, Eskandari S, Kaznessis YN, Sherman MA, Waring AJ. Conformational mapping of the N-terminal peptide of HIV-1 gp41 in lipid detergent and aqueous environments using ^{13}C-enhanced Fourier transform infrared spectroscopy. *Prot. Sci.* 2004; **4**: 1012–1030.
9. Gao X, Wong TC. Abstract: Molecular dynamics simulation of adrenocorticotropin (1-10) peptide in a solvated dodecylphosphocholine micelle. *Biopolymers* 2001; **58**: 643–659.
10. Wymore T, Wong TC. The structure and dynamics of ACTH (1-10) on the surface of a sodium dodecylsulfate (SDS) micelle: a molecular dynamics simulation study. *J. Biomol. Struct. Dyn.* 2000; **18**: 461–476.
11. Brooks BR, Bruccoleri RE, Olafson BD, States DJ, Swaminathan S, Karplus M. CHARMM: A program for macromolecular energy, minimization, and dynamics simulations. *J. Comp. Chem.* 1983; **4**: 187–217.
12. Jorgensen WL, Chandrasekhar J, Medura JD, Impey RW, Klien ML. Comparison of simple potential function for simulating liquid water. *J. Chem. Phys.* 1983; **79**: 926–935.
13. MacKerell A. Molecular dynamics simulation analysis of a sodium dodecyl sulfate micelle in aqueous solution: decreased fluidity of the micelle hydrocarbon interior. *J. Phys. Chem.* 1995; **99**: 1846–1855.
14. Andersen HC. Molecular dynamics simulations at constant pressure and/or temperature. *J. Chem. Phys.* 1980; **72**: 2384–2393.
15. Essman U, Perera L, Berkowitz ML, Darden T, Lee H, Pederson LG. A smooth particle mesh Ewald method. *J. Chem. Phys.* 1995; **103**: 8577–8593.
16. Ryckaert JP, Ciccotti G, Berendesen HJC. Numerical integration of the cartesian equations of motion for a system with constraints: Molecular dynamics of n-alkanes. *J. Comp. Phys.* 1977; **23**: 327–341.
17. Kamath S, Wong TC. Membrane structure of the human immunodeficiency virus gp41 fusion domain by molecular dynamics simulation. *Biophys. J.* 2002; **83**: 135–143.
18. Mobley PW, Pilpa R, Brown C, Waring AJ, Gordon LM. Membrane-perturbing domains of HIV type 1 glycoprotein 41. *AIDS Res. Hum. Retroviruses* 2001; **17**: 311–327.
19. Chang D-K, Cheng S-F. Determination of the equilibrium micelle-inserting position of the fusion peptide of gp41 of human immunodeficiency virus type 1 at amino acid resolution by exchange broadening of amide proton resonances. *J. Biomol. NMR* 1998; **12**: 549–552.